Constitutive law BETON_REGLE_PR

Summarized:

This documentation presents model BETON_REGLE_PR established by company NECS in the frame of the free community Code_Aster. It is about a lawful model [bib1], written by combining two models 1D.

Contents

1 Presentation of model BETON_REGLE_PR3
2 Description of the variables internes4
3 Validation4
4 Bibliographie4
5 Description of the versions of the document4

1 Presentation of model BETON_REGLE_PR

the constitutive law are of type "twice 1D" in the clean reference of strain (confused with the clean reference of stress). One 1D describes only one behavior, which is of elastic type nonlinear.

In compression, it is the model right-angled parabola in the regular manner definite [bib1]; the stress is given by the following relations:

$$\sigma=\sigma_y^c\left[1-\left(1-\frac{\varepsilon}{\varepsilon_0}\right)^n\right] \quad \text{if } 0<\varepsilon\leq\varepsilon_0 \text{ (parabola part)} \qquad \textbf{éq.1}$$

$$\sigma=\sigma_y^c \quad \text{if } \varepsilon>\varepsilon_0 \text{ (left right-angled)}$$

In tension the model is of standard triangle [bib2]:

$$\sigma=E\varepsilon \quad \text{if } \varepsilon\leq\frac{\sigma_y^t}{E} \qquad \textbf{éq.2}$$

$$\sigma=\sigma_y^t+E_T\left[\varepsilon-\frac{\sigma_y^t}{E}\right]$$

the materials parameters associated ones are the following:

E : Young modulus;
σ_y^t : the stress with the peak in tension (f_t);
E_T : the tangent modulus (generally equal to $\frac{-E}{10}$);
σ_y^c : the maximum stress in compression (f_c);
n : the exhibitor of the model of hardening in compression;
ε_c : the strain to which one reaches σ_y^c .

The response stress-strain is given on the following figure:

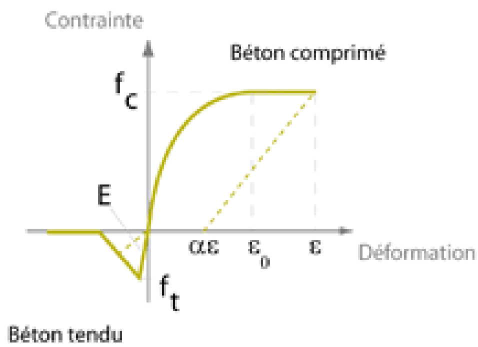

Appear 1-a: stress-strain curve in 1D

2 Description of the local variables

It does not have there a local variable for this model.

3 Functionalities and validation

3.1 Functionality

the model is available only in 2D and is thus accessible with modelizations D_PLAN, C_PLAN and DKT.

3.2 Validation

the validation of the model was made by comparison with the experimental results got on a reinforced concrete slab subjected to its inertia loadings and a pressure in the center of the slab [bib1]. The ratio written by NECS was placed in Appendix. The constitutive law can be defined by the key word BETON_REGLE_PR (command STAT_NON_LINE, key word factor COMP_INCR). It is associated with material BETON_REGLE_PR (command DEFI_MATERIAU).

Model BETON_REGLE_PR is checked by the case following test:

SSNP129	[V6.03.129]	Validation of model ETON_REGLE_PR on an element DKT

4 Bibliography

1.BAEL 91 revised 99 (NF P 18-702)
2.VB. Zhang, *R. Masmoudi, B. Benmokrane, Behavior of one-way concrete slabs reinforced with CFRP grid reinforcements, Constructions and Materials Buildings, 18, pp. 625-635*, 2004

5 Description of the versions of the document

Version Aster	Author (S) Organization (S)	Description of the modifications
11.3	S. Michel-Ponnelle EDF-R&D/AMA	initial Text

Annexe 1

Validation of constitutive law `BETON_REGLE_PR`
(Note NECS N°S&M_RA_1_06)

1. OBJET

the ratio presented here will attempt to validate a slab computation realized via software CADABA by comparison with experimental results. The purpose is double: apart from the capacity of the model to reproduce the test, a stress will be laid on the sensitivity to the spatial discretization of the mesh finite element used, to the strength criteria of the materials and the representativeness of materials parameters associated. It is thus a question of proposing a case complete test of validation making it possible to evaluate the reliability of the software for the reproduction of a reinforced concrete slab computation.

2. METHODOLOGY

2.1 description of slab

One is based, for this work, on the results got in [1]. One considers a reinforced concrete slab of dimensions $3\mathrm{m}\times 1\mathrm{m}\times 0{,}25\,m$ (Figure 1). The structure is reinforced by steels (category 400, number 15) of section $200\,mm^2$ (diameter $16\,mm$) for the tended zone (low three-dimensions function) and by steels of section $28\,mm^2$ (diameter 6 mm) for the compressed zone (high three-dimensions function) and distributed as indicated in Figure 2. For the needs for computation, the distributions of steel are then converted of density per linear meter. All the properties are summarized in Table 1.

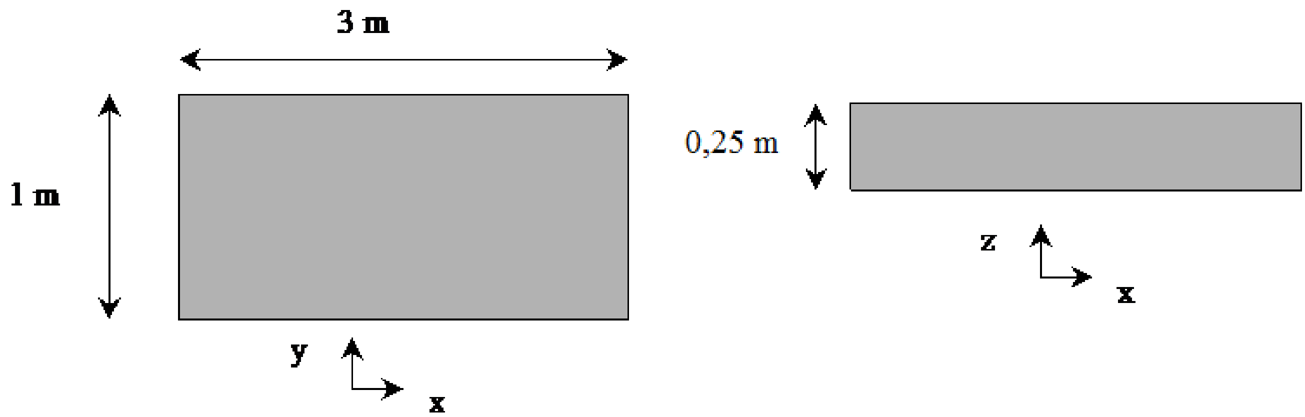

Figure 1. Geometry of slab considered

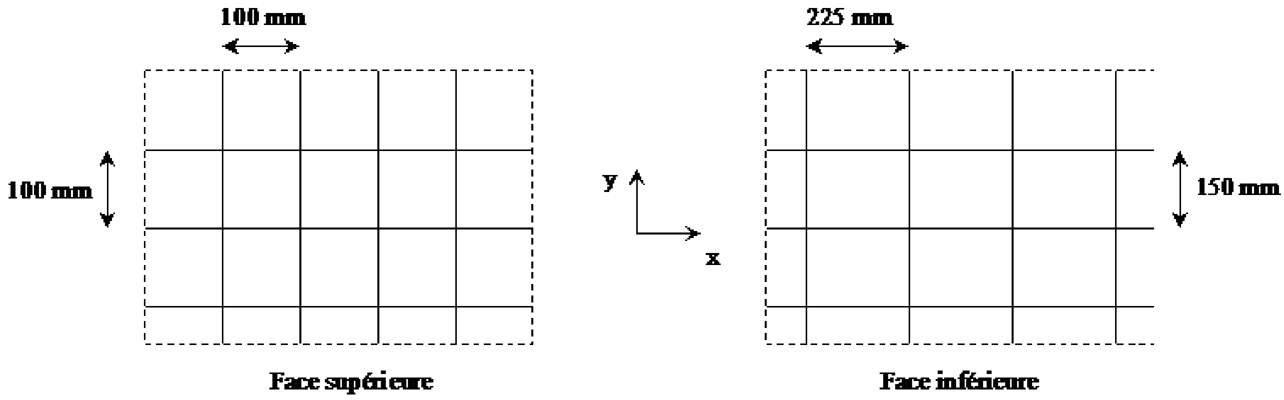

Figure 2. Distribution of steels in slab. Compressed zone (on the left) and zones tended (on the right)

Face supérieure (près de Z max)	
Armatures parallèles à XX	
Section d'armatures (cm ²/ml) *Section unique sur toute la longueur*	2,8
Armatures parallèles à YY	
Section d'armatures (cm ²/ml) *Section unique sur toute la longueur*	2,8
Face inférieure (près de Z min)	
Armatures parallèles à XX	
Section d'armatures (cm ²/ml) *Section unique sur toute la longueur*	14
Armatures parallèles à YY	
Section d'armatures (cm ²/ml) *Section unique sur toute la longueur*	8,9

Table 1 Characteristics of steels

One considers for the three-dimensions functions of reinforcement a coating of $38\,mm$ (high three-dimensions function located at $0{,}084\,m$ average average, low three-dimensions function located at $0{,}079\,m$ average average).

2.2 loading

the slab is posed on two fixed linear bearings and is subjected to two distinct loadings:

- its inertia loading corresponding to a total load of $18{,}75\,kN$ (distributed pressure of $6{,}25\,kN.m^{-2}$)
- the second loading is a pressure uniformly distributed on a rectangular surface in the center of slab of dimensions $300\,mm \times 300\,mm$ (Figure 3). This force is applied in the direction of z negative (negative deflection) and its intensity is monotonous variable.

The slab is charged until plasticization with steels and crushing of the concrete. The strain in the concrete measured is then of 3 $^{0/00}$, and 7,5 $^{0/00}$ in tended steel. The measured deflection is of $34\,mm$. The end of the tests is marked by the crushing of the compressed concrete.

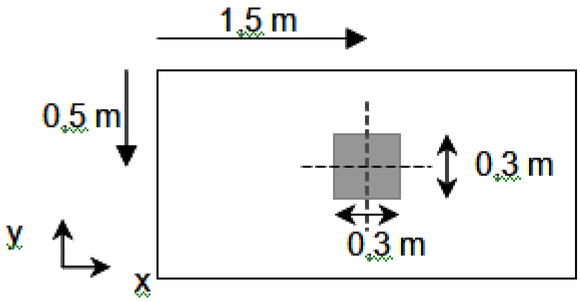

Figure 3. Diagram of application of force

3. Modelization

3.1 Boundary conditions

the boundary conditions applied are given in Table 2. They are selected so as to remain most representative possible of the experimental test.

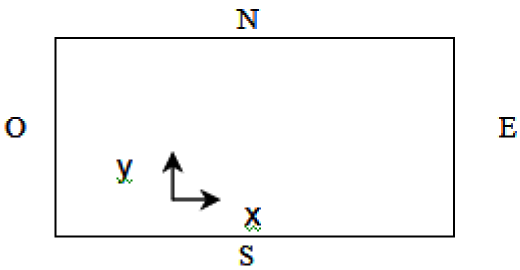

The axis z is located in the direct reference (outgoing axis of the plane xy). The grayed boxes indicate that these degrees of freedom are automatically left free by the software

Bord	E	O	N	S
	//yy	//yy	//xx	//xx
Déplacement suivant X	libre	libre	libre	libre
Déplacement suivant Y	libre	libre	libre	libre
Déplacement suivant Z	bloqué	bloqué	libre	libre
Coin	N-O	S-O	N-E	S-E
Déplacement suivant X	libre	bloqué	libre	libre
Déplacement suivant Y	libre	bloqué	libre	bloqué

Table 2. Boundary conditions.

3.2 materials parameters

materials parameters are defined starting from the data in [1]. They will thus be useful basic for computations on slab. The constitutive laws of steel and the concrete are selected starting from the opportunities given by the software.

The behavior of the concrete is that defined by the model “parabola-rectangle” in accordance with the provisions of regulation BAEL [2] concerning the compressed part of the material. The tended part is modelled by the “triangular” model [3] (Figure 4).

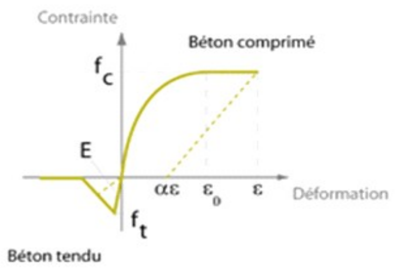

Figure 4. Model parabola – rectangle for the compressed concrete and triangle for the tended concrete.

The characteristics are in the following way defined:

Young modulus	E : 37 000 MPa
Peak of stress compressive	f_c : 45 MPa
Strain with the peak of stress compressive	ε_0 : 1,2 $^{0/00}$
Peak of stress tensile	f_t : 3,9 MPa
Exhibitor of the model parabola-rectangle	n : 2
Unrecoverable deformation a:	50%

the behavior of reinforcements leaves is that defined by the bilinear classical model (elastoplastic with linear kinematic hardening) [3] (Figure 5).

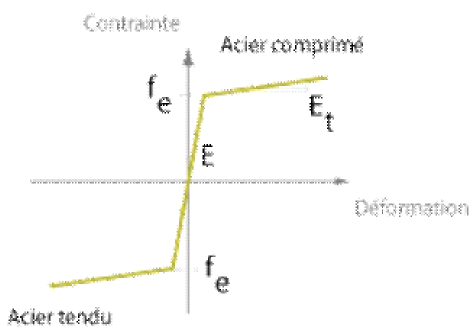

Bilinear figure 5. model for the steel reaction of

the characteristics measured on the basis of test of characterization of laboratory are in the following way defined:

Limit of plasticization	f_e : $540\,MPa$
Young modulus	E_a : $195\,000\,MPa$
Slope of hardening	E_T : $1\,000\,MPa$ *

the stopping criteria for computation are:

- a maximum strain in the concrete of 5 0/00 **
- or a maximum strain in the steel of 25 0/00 ***

* the article [1] does not provide a curve of behavior resulting from tests of characterization of reinforcements. It is thus not possible to indicate to just the tangent modulus after plasticization. This value was selected on the basis of our experiment.

** The article [1] does not provide an indication for the rupture limit of the concrete in compression. This value was chosen by Séchaud & Metz.

*** This value was chosen by Séchaud & Metz.

3.3 discretization

the structure is discretized in the case of reference with 300 nodes and 11 layers in the thickness. The mesh obtained is given in Figure 6.

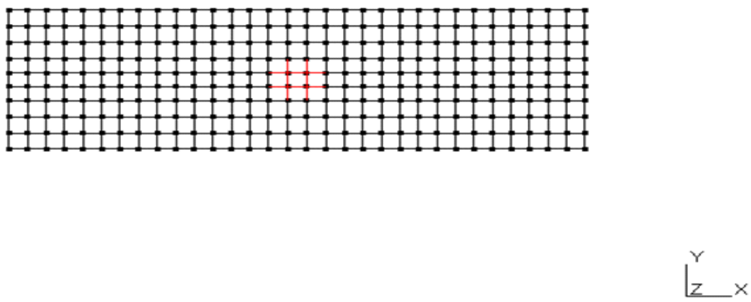

Figure 6. Mesh of reference of slab

4. Analytical computation of the Yield-point load

One calculates the Yield-point load supported by slab by considering the burden-sharing given in Figure 7.

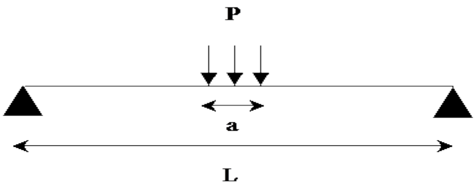

Figure 7. Distribution of the loading for the computation of the Yield-point load

the maximum moment is calculated in the center and is worth:

$$M_{max} = P(\frac{L}{4} - \frac{a}{8})$$

d'où :

$$P_{res} = \frac{M_{res}}{(\frac{L}{4} - \frac{a}{8})}$$

avec la géométrie du problème, on obtient :

$$P_{res} = 1.4 M_{res}$$

avec :

$$M_{res} = 0.27132 f_e$$

d'où

$$P_{res} = 0.38 f_e$$

For an elastic limit $f_e = 400\,MPa$, one obtains a value of $152\,kN$ and $205\,kN$ for a limit of $540\,MPa$. This interval is in agreement with the experiment which gives a point of plasticization of steels of approximately $180\ kN$.

5. LAYERS

computations are carried out with the calculation programme CADABA version 2.0.8. The basic core of the solver is *Code_Aster*® 7.3.10.7 version - NECS.

6. ANALYZES RESULTS

Various computations were realized and are summarized in Table 3. The following paragraphs will attempt to exploit these results and to give conclusions. The curved applied force – deflection in the center will be used as reference for these comparisons.

Number of test	Many nodes	Eb (MPa)	FC (MPa)	E_0	ft (MPa)	N	Fe (MPa)	Ea (MPa)	AND (MPa)
1.300		37.000	45.1,2. 3,9			2. 54 0. 19 5		000	1.000
2.600		37.000	45.1,2. 3,9			2. 54 0. 19 5		000	1.000
3.150		37.000	45.1,2. 3,9			2. 54 0. 19 5		000	1.000
4.300		37.000	45.1,2		2	2. 54 0. 19		000	1.000

						5			
5.300		37.000	45.1,2		2	2.540.180		000	1.000
6.300		37.000	45.1,2		2	2.520.180		000	1.000
7.300		37.000	45.1,2		2	2.500.180		000	1.000
8.300		37.000	45.1,2		2	2.500.180		000.500	
9.300		37.000	45.1,2		0	2.500.180		000	1.000
10.150		37.000	45.1,2		2	2.500.180		000	1.000
11*	60	37.000	45.1,2		2	2.500.180		000	1.000

Table 3. Synthesis of the various cases of simulation by CADABA

For the case n°11 the surface of application of the load was also modified (of 30x30 cm to 55x50 cm) to take account of the distribution of the stresses towards the average average of slab, in agreement with the regulations of the B.A.E.L. (§ A.3.2.5). 6.1

quality control of the mesh

cases 1,2 and 3 make it possible to check the quality of the model and the sensitivity of the response obtained according to the mesh. The comparison between cases 1,2 and 3 is given in Figure 8. Only the number of nodes of the spatial discretization evolves. From

a general point of view, the smoothness of the spatial discretization, in the beach of values considered here, affects only little the quality of the results. Only the stagnation point of the curves differs, the paces qualitative (elasticity, plastic bearing and tangent modulus) and quantitative (same values of the reaction for the same deflection) remain the same ones. That

thus makes it possible to check the quality of the model. The variations observed on the stagnation point come owing to the fact that the algorithm of control of computations does not aim to step at refining the increments of loading to stop computations closest to the going beyond of criterion. The increments of load are estimated by other considerations, and the computations stop when the last point exceeds at least one of the thresholds of fracture (steel, concrete, rotation of the hinges). Moreover, although they are weak in this case, case the strains obtained by the models are slightly function of the size of meshes selected. Figure

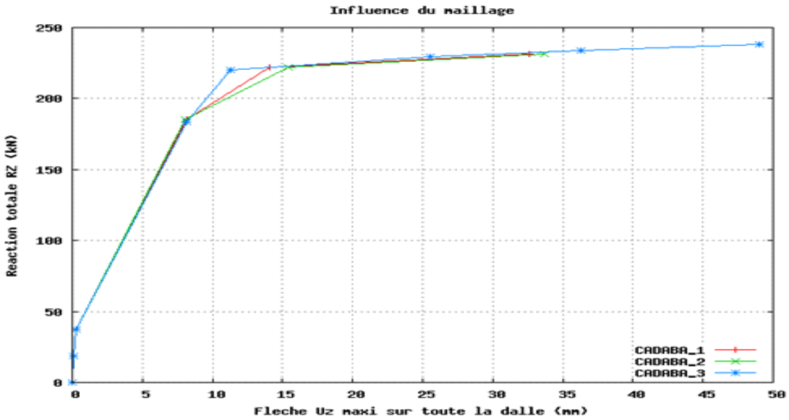

8. Influence mesh 6.2

influences strength in tension of the concrete Taking into account

the little of dependence on the discretization observed on these total results, one will use in the rest of this document a mesh with 300 nodes. Considering the relative distance between the experimental response and the simulations using the parameters of reference, one studies the influence of strength in tension of the concrete. For that, cases 1 and 4 are compared. Figure

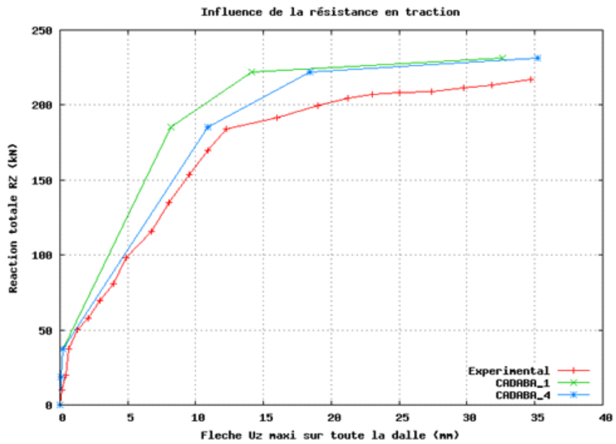

9. Influence strength in tension of the concrete To decrease

strength in tension of the concrete allows to obtain a stiffness after cracking closer to the experimental test. This reduction, compared to the experimental data, can be justified taking into account the difficulty of precisely evaluating strength in tension of a concrete (theoretical value of computation equalizes with, to see $0\,MPa$ paragraph 6.6). For a better retiming of the curves it is also possible to identify the best value for the parameter e0 (cf Table 3). 6.3

influence of the Young modulus of steel Taking into account

the effect of strength in tension of the concrete, one takes for new value of. f_t One $2\,MPa$ evaluates now the influence of the Young modulus of steel (comparison of cases 4 and 5, cf Figure 10). Figure

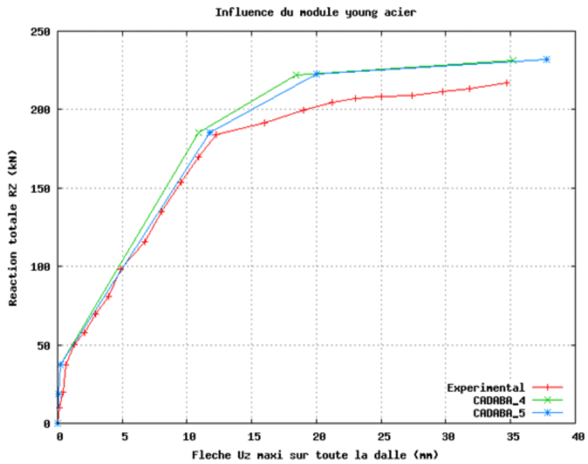

10. Influence Young modulus steel To decrease it

the Young modulus of the steel of less than 10% allows to approach the experimental response more precisely. This modification of the values of reference remains acceptable taking into account uncertainties of measurement on the parameter. 6.4

influence of the threshold of plasticization of steels Taking into account

the preceding study, strength in tension of the concrete is selected with and it $2\ MPa$ Young modulus of steel with. One $180\,000\ MPa$ studies

now the influence of the threshold of plasticization of steel (case 5,6 and 7, cf Figure 11). The reduction in the threshold of plasticization of steels makes it possible, by definition, to reveal the last mode of behavior (response of structure directed by the stiffness of steel only) earlier. Figure

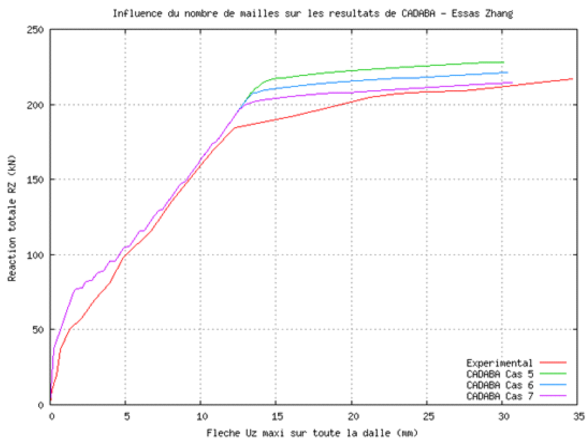

11. Influence threshold of plasticization of steels In

our case, it becomes thus possible to approach the experimental response more precisely. According to whether one seeks as well as possible to fix the force of plasticization of reinforcement, or the level of ultimate tensile strength (bearing capacity of slab) the limiting value of plasticization of reinforcement can be estimated enters and 450 . 6.5 $500\ MPa$

influence of the tangent stiffness Taking into account

the preceding comparison, strength in tension is selected with, $2\ MPa$ the Young modulus of steel with and $180000\ MPa$ the threshold of plasticization of steels with. One $500\ MPa$ studies now the influence of the tangent stiffness of steel (case 7,8, cf Figure 12). The tangent

stiffness of steel controls the last mode of behavior of structure. It thus makes it possible as well as possible to gauge the final slope of the curve forces – deflection. In our case, the value initially selected seems the good choice to be preserved. 6.6

comments on the classical parameters One wishes

here to compare the experimental response with the criteria classically retained for reinforced concrete slabs. In particular, one null considers a strength in tension of the concrete (case 9) and one it compared to the experimental response and with his best approximation (case 7) (Figure 13). For this precise case, the taking into account of a strength in tension null for the concrete has little influence on the simulated response. It is noted that to modify strength in tension of the concrete especially a modification induces on the initial behavior of the material (Figure 14) (phenomenon not observed in Figure 9 taking into account the discretizations of loading obtained). Figure

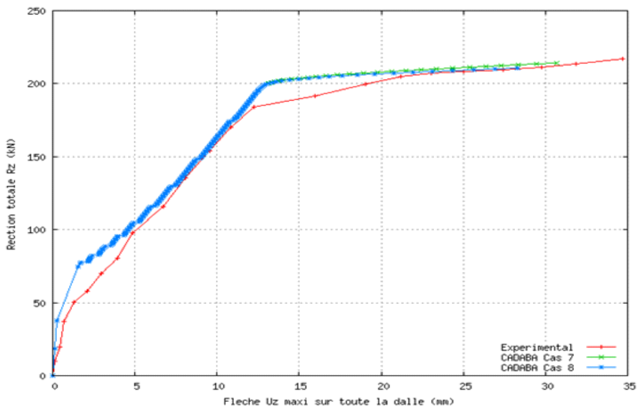

12. Influence tangent stiffness of steel Figure

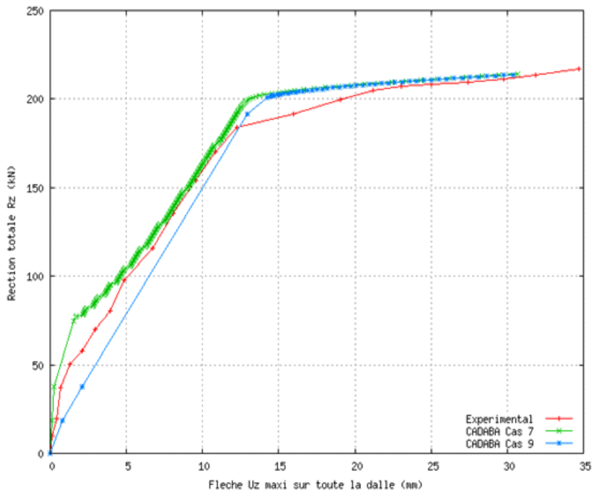

13. Taking into account of a strength in tension null for the concrete. Figure

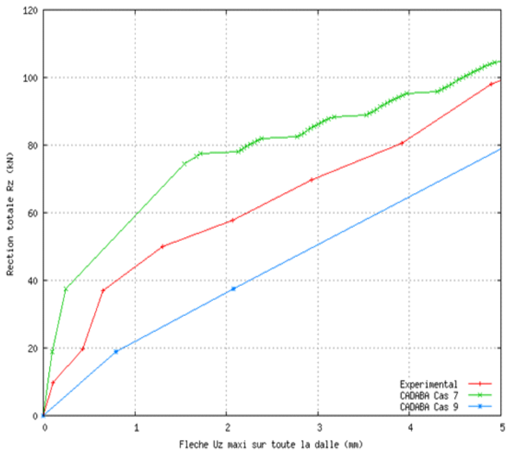

14. Zoom on the initial part of the curve. However

the influence of this choice on the bearing capacity of slab is less important. Indeed, apart from the contribution of the slightly tended layers, and the evolution height of the neutral axis, the effects on strength of the section of slab are rather negligible. 6.7

local results (strains) Concerning

the ultimate state, and the fracture of the materials, in the end of the simulation of case 7 one observes the following results (with the simulation of Figure 16 container more points of comparison): eminbéton

compressed = -3,16 0/00 Stopping criteria = -5 0/00 emaxacier

tightened = 26.16 0/00 Stopping criteria = 25 0/00 This

indicates that computations stopped by the going beyond the threshold of fracture of steels. The authors of [1] noted a stop of the test by plasticization of the tended steels followed by a fracture of structure by compression of the concrete. By considering the ultimate strain of the concrete close to more classical value for the static situations, of 3 0/00 (last point of the experimental curve), one notices that the two limits are thus reached simultaneously. However

the local results (strains) got by a simulation by EF depend on the spatial discretization. As information Table 4 and figure 15 indicate the level of these variations. It is thus essential to adopt dimensions of finite elements making it possible to restore realistic strains in the materials. The curves of Figure 15 compare the evolution of the strains of the concrete and steel with the levels of request. The observations which one can draw are on the one hand related to simulations only, and on the other hand with the comparison with experimental measurements. The curves correspondings with Cases 7,10 and 11, where only the mesh was modified, indicate that as from the moment when degradations are accentuated and concentrated on part of the model, the amplitude of local measurements grow conversely in keeping with meshes. Concerning the comparisons with experimental measurements it should be recalled that these measurements were carried out in a fixed point of structure. The heterogeneous nature of the concrete and the distribution of cracks make not easily exploitable of the specific observations to weak sample. Indeed it is enough that a macro-crack through structure with the right of a gauge, or a few millimetres so that measurements appear very varied. It is besides for this reason that in the mode before localization of the damages all the curves coincide. Concerning
the strains in steels, the best correlation between computation and the tests is obtained for case 11, where the size of meshes is of the same order as the thickness of slab. Concerning the strains of the concrete, there remains a variation enters the model and the test. This variation can be explained by the fact why in the enforcement zone of the load, of the localised stresses due to the application of the load superimpose themselves on the stresses due to the bending of slab, and that this local phenomenon is not represented in the modelization in shells. maximum

			strains obtained for a deflection of Nbr $30\,mm$	
Mesh.	nodes Cuts	smaller mesh E min	compressed concrete E max	steel tightened case
7 300	9,6	cm -3,0	0/00 25,4	0/00 case
10.150	15,0	cm -2,2	0/00 17,5	0/00 case
11 60 25,0		cm -1,5	0/00 10,7	0/00 Table

4. Influence size of meshes EF on the local results necessary to the determination of the numerical failure of the models Figure

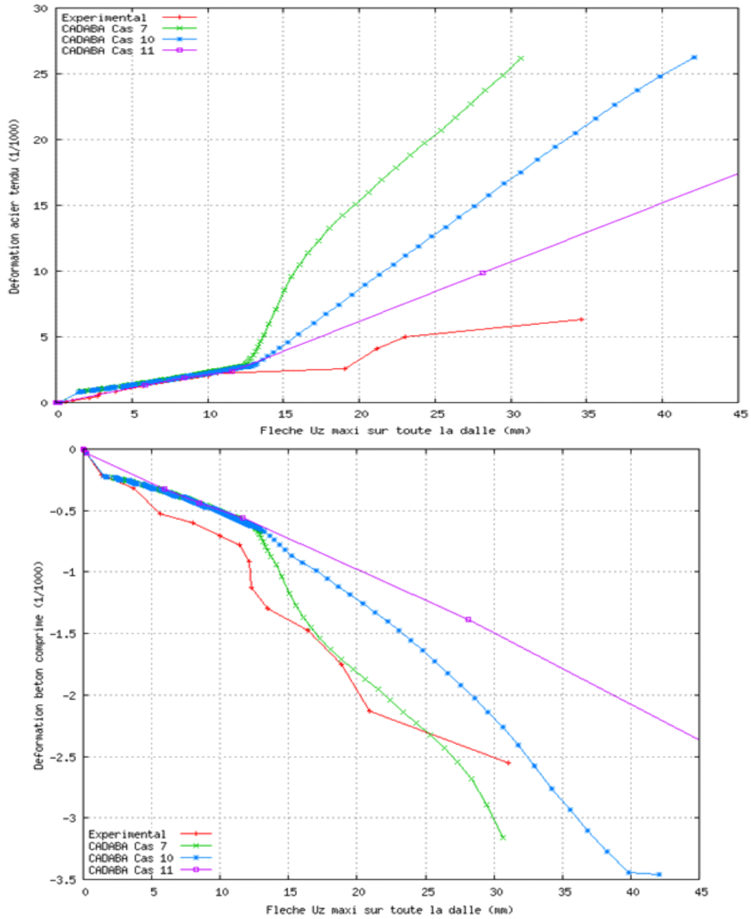

15. Evolution of the steel and concrete strains recorded during the test. 7.

CONCLUSIONS In conclusion

, these various computations allowed: to show

- the objectivity of simulation compared to the spatial discretization. to show
- the capacity of CADABA to reproduce reinforced concrete an experimental slab test. Concerning this purpose, case 6 is retained like the best chock (Figure 16). The modifications of materials parameters compared to the experimental reference are acceptable (less than 10%) taking into consideration available data, and the conditions of characterization of the mechanical parameters (standardized tests, size of the test-tubes, methods of measurement, etc). to highlight
- the sensitivity of the local results necessary to the determination of the ultimate state of strength of materials. The choice of sizes of meshes close to the thickness of slab makes it possible to be freed from this skew. Obviously

it is possible to reach chocks even finer, however the goal of this work is not to obtain a perfect chock between simulation and the test, but to more show that the mechanical ingredients integrated into the tool for simulation can provide a reasonable estimate of the behavior of a slab, with data files materials close to values standards. Figure

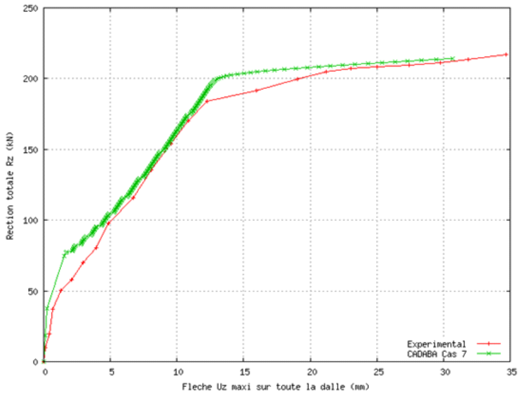

16. Comparison assai/CADABA with the sets of parameters retained (case 7) 8.

DOCUMENTS OF REFERENCE B. Zhang

1 , R. Masmoudi, B. Benmokrane, Behavior *of one – way concrete slabs reinforced with CFRP grid reinforcements, Constructions* and Materials Building, 18, pp. 625-635, 2004 BAEL

2 91 revised 99 (NF P 18-702)